



Contents lists available at ScienceDirect

Bioorganic & Medicinal Chemistry

journal homepage: www.elsevier.com/locate/bmc

Anti-atherosclerosis effect of H₂S donors based on nicotinic acid and chlorfibrate structures

Zhongjie Bai^a, Jinlong Zhang^a, Qiuping Zhang^a, Yanni Wang^a, Jili Li^a, Quanyi Zhao^{a,*}, Zhen Wang^{a,*}, Dian He^a, Jingke Zhang^b, Bin Liu^c

^a Institute of Medicinal Chemistry, School of Pharmacy of Lanzhou University, Lanzhou 730000, China

^b GLP Lab Centre, School of Basic Medicine of Lanzhou University, Lanzhou 730000, China

^c School of Stomatology of Lanzhou University, Lanzhou 730000, China

ARTICLE INFO

Keywords:

H₂S donors
Toxicity
Anti-atherosclerosis effect
Anti-inflammatory
Anti-oxidation effect

ABSTRACT

Based on the structures of nicotinic acid and chlorfibrate, a series of new H₂S donors were synthesized and their anti-atherosclerosis activities using Ox-LDL RAW 264.6 cells as model were evaluated. The release test showed that all the compounds could release H₂S effectively and showed low cytotoxicity. In the bioactivity experiments, compounds 1, 3, 9 and 14 increased the survival rate of HUVEC cells treated by ox-LDL; among four compounds, compounds 1 and 3 displayed higher activity than the others. In the foam cell model, compounds 1 and 3 were found to inhibit the formation of foam cells and significantly reduced the content of TC and FC in foam cells. They had more obvious effects on lipid reduction than those of nicotinic acid and chlorfibrate. In anti-oxidation, compounds 1 and 3 significantly reduced ROS and MDA and increased the expression level of SOD, whereas the precursor compounds, niacin and chlorfibrate had little antioxidant effect. In addition, both compounds also inhibited the inflammatory response in foam cells, with reducing pro-inflammatory factor TNF- α and increasing anti-inflammatory cytokine IL-10. WB assay showed that the tested compounds inhibited the expression levels PI3K, Akt and NF- κ b proteins. In conclusion, the compounds as H₂S donors could protect HUVEC cells from damage and inhibit the formation of foam cells by inhibiting PI3K/Akt/NF- κ b signal pathway. All these suggest the compounds have potential to be candidate for anti-atherosclerosis medicines.

1. Introduction

Atherosclerosis (As) is a vascular disease which characterized by plaque formation on the endothelial wall, causing hardening and narrowing of arteries. The process of atherosclerosis is initiated by accumulation of fatty materials such as cholesterol and triglyceride,¹ and it involves in multiple cell types, mediators and a combination of pathogenic factors including chronic inflammation, endothelial dysfunction and oxidative stress.^{2–4}

Hydrogen sulfide (H₂S) is a gasotransmitter like nitric oxide (NO) and carbon monoxide (CO).⁵ Similar to nitric oxide, H₂S is a potent vasodilator^{6,7} and possesses vasoprotective effects, such as reduction of VSMC proliferations.⁸ Many testing results showed H₂S played an important role to inhibit the factors which giving rise to atherosclerosis. Deficiency of H₂S appeared to accelerate atherosclerosis. For example, CSE-knockout mice were found to develop early fatty streak lesions in the aortic root. The plasma levels of cholesterol and low-density lipoprotein cholesterol elevated, and lesional oxidative stress and adhesion

molecule expression increased.^{9,10} On the contrary, supplementation with H₂S inhibited atherosclerosis. In ApoE knockout mice, H₂S inhibited ICAM-1 expression in TNF- α induced HUVECs via the NF- κ B pathway,¹¹ and up-regulated SOD expression accompanied by a reduced level of ROS.¹² H₂S also inhibited macrophage infiltration and reduced lesion size by down-regulation of CX3CR1 and CX3CL1 in macrophages.¹³ Furthermore, H₂S also inhibited H₂O₂ mediated mitochondrial dysfunction in human endothelial cells and attenuated TNF- α induced inflammatory signaling and dysfunction in vascular endothelial cells.^{12,14}

Since H₂S is gas and its dose uncontrollable, H₂S donor is one of the substitutes.¹⁵ Among them, NaHS has been widely used to evaluate the biology of H₂S and has provided useful information about the pharmacological effects of this gas. However, NaHS releases a large amount of H₂S in a short period of time, which causing tissue cells toxic damage.¹⁶ Recently, GYY4137, a classic H₂S donor, was found to inhibit lipid accumulation induced by ox-LDL in RAW 264.7 cells. In vivo, GYY4137 decreased vascular inflammation and oxidative stress,

* Corresponding authors.

E-mail addresses: zhaogy@lzu.edu.cn (Q. Zhao), zhenw@lzu.edu.cn (Z. Wang).

<https://doi.org/10.1016/j.bmc.2019.06.012>

Received 15 March 2019; Received in revised form 2 June 2019; Accepted 5 June 2019

0968-0896/© 2019 Elsevier Ltd. All rights reserved.

improved endothelial function and reduced atherosclerotic plaque formation in ApoE knockout mice.¹⁷ Therefore, H₂S donors have a big potential to be as anti-atherosclerosis molecules.

However, there are many factors in the progression of atherosclerosis. Among them, hyperlipidemia is one of the main factors.¹⁸ Niacin and clofibrate are hypolipidemic agents in clinic, and have effect of preventing atherosclerosis. Combined with Niacin (or clofibrate) through the ester bond, the H₂S donors will be pro-drugs. They will be hydrolyzed into antilipidemic drugs and H₂S donors *in vivo* under the action of esterase, which taking synergistic effects to effectively alleviate the symptoms of atherosclerosis.

Based on the theory, in this paper, we have synthesized the H₂S donors based on niacin or clofibrate, and evaluated their effect of anti-atherosclerosis using Ox-LDL RAW 264.7 cells as model, including the effect of compounds on the formation of foam cells, the intracellular lipid accumulation; meanwhile, ROS and MDA levels were measured. By which, we hope to provide a basis for whether it has a value to further study.

2. Results and discussion

2.1. Synthesis and characterization

Based on the structure of nicotinic acid and 2-(4-Chlorophenoxy)-2-methylpropionic acid, eighteen compounds were synthesized. Among them, compounds 1–8 were synthesized from (±)-α-lipoic acid, TBZ and ADTOH. However, compounds 9–18 introduced into the COS/H₂S donor as the latest reported.¹⁹ The synthesis of compounds 1–3 and compounds 9–18 is carried out in two steps, which are obtained by splicing an acid and a releasing group with 1, 3-propanediol and ethanolamine, respectively (Schemes 1–3). The intermediate products are all yellow oil.

The spectra of all compounds correspond with the expected. In IR spectra of all compounds, there has a strong absorption peak at in range of 1728–1766 cm⁻¹, which is the characteristic absorption of ester C=O. Strong peak appeared in 1120–1181 cm⁻¹ is the absorption bands for C=S. The signals of C–S bond appeared in 604–624 cm⁻¹. In ¹H NMR spectra, the benzene ring H signals appeared at 6.70–7.89 ppm. The signals appeared at 3.53–5.23 ppm is methylene H. In ¹³C NMR spectra, the signals of C=O appeared in 161.42–172.85 ppm. All compounds are insoluble in water, and easily dissolve in organic

solvents, like DCM, THF, DMSO, and so on.

2.2. H₂S releasing test of compounds

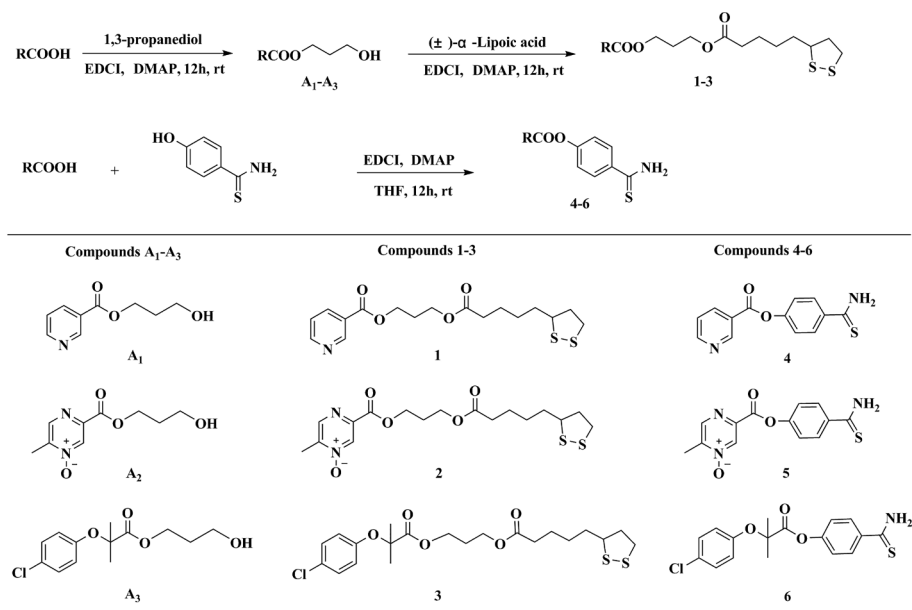
The H₂S release ability of compounds 1–18 was measured by methylene blue method.²⁰ Results as shown in Table 1, all the compounds released H₂S under the testing condition. The maximum release of compounds 1–3 were significantly higher than those of other compound. Compound 1 released H₂S 41.4 μM at most. Among all the compounds, the half-life of compound 3 was longest, and it was 21.3 min. However, for compounds 9–14 contain O–C=S group, they all released H₂S fast, and their half-lives were not up to 2 min. Among them, compound 13 was the fastest H₂S releaser, and its t_{1/2} only 0.8 min. The release rate was closely related to the electronegativity of substituent on the thioisocyanate benzene ring; and the stronger the substituent electron withdrawing ability, the faster the hydrogen release rate. In contrast, compounds 1–3 are more suitable for further bioactivity study due to its larger release of H₂S and its relatively slow rate.

2.3. Cytotoxicity of the compounds

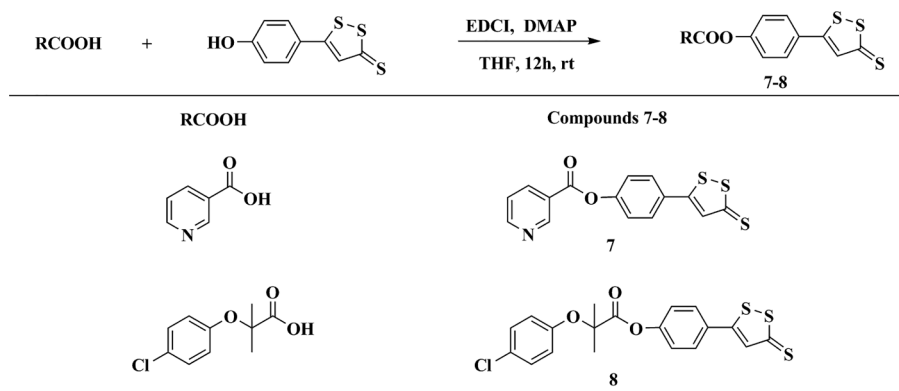
Before studying activity, we first evaluated the cytotoxicity of these compounds to four cell lines by MTT method, and obtained their IC₅₀ values. Results as shown in Table 2, compounds 1–3 did not display any antiproliferative effect against H9c2, HUVEC, RAW264.7 and W138 cells, the IC₅₀ values were all > 800 μM. Compounds 4–18 also showed almost no toxicity to RAW264.7, but they displayed more or less slightly toxic for the other three cell lines. As for HUVEC cells, their IC₅₀ values were beyond 500 μM; for example, the IC₅₀ values of compounds 7 and 13 were 562.3 μM and 549.6 μM, respectively. In summary, all the compounds have very low cytotoxicity, which do not affect the testing results of bioactivity in following.

2.4. Protective effect of compounds on HUVEC injury induced by ox-LDL

Vascular endothelial cell injury often leads to endothelial dysfunction, and it is closely related to the occurrence and development of cardiovascular diseases such as atherosclerosis.²¹ Ox-LDL is an important factor in the pathogenesis of atherosclerosis (As).²² It not only induces macrophage to form foam cells, but also damages endothelial



Scheme 1. The structures and synthetic route of compounds 1–6.



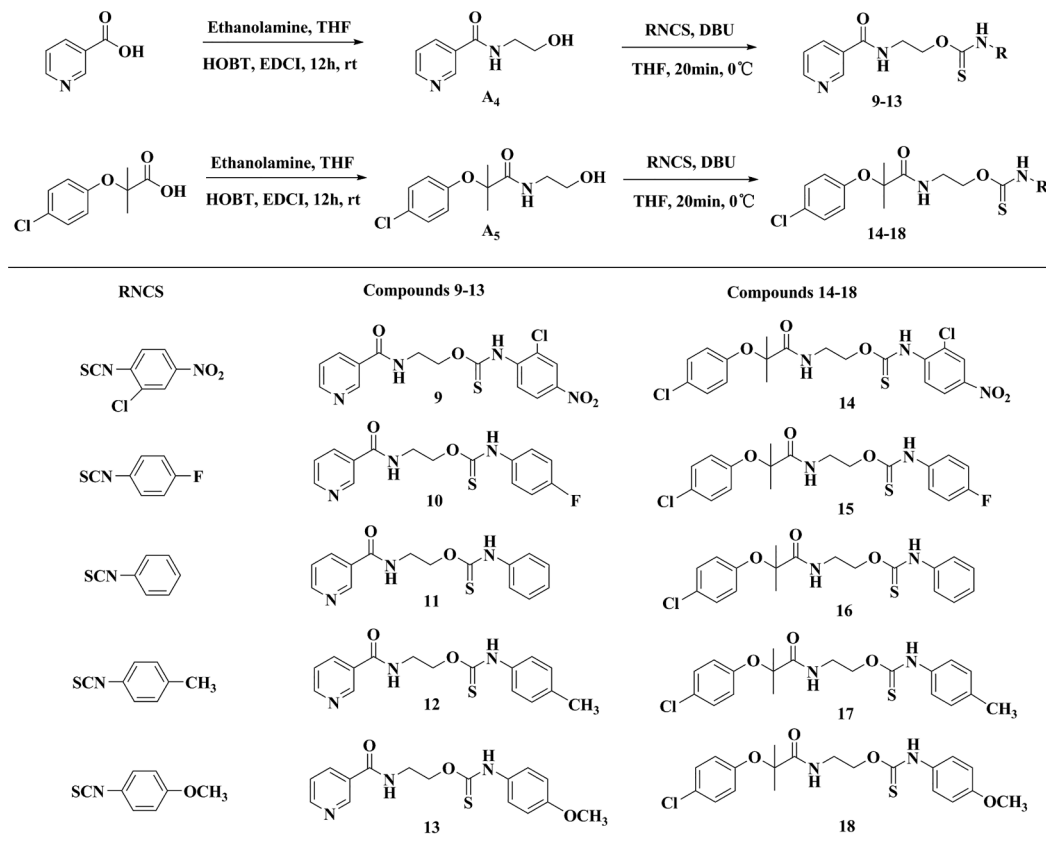
Scheme 2. The structures and synthetic route of compounds 7–8.

and finally makes plaque accumulation in vascular lumen. H_2S displayed vasoprotective effects and inhibited VSMC proliferations.²³ So, we think these compounds as H_2S donors possibly have a protection to endothelial cells. To confirm our thought, we chose HUVEC cells treated with ox-LDL as model, and the survival rate of HUVEC cells was firstly measured in the presence of H_2S donor. As shown in the Fig. 1, the tested compounds (1, 3, 9 and 14) have almost no effects on the survival rate of HUVEC cells in the range of 10–100 μM . After treated with ox-LDL, the survival rate of HUVEC cells reduced to 73.1% compared with the control group (Fig. 2). This suggests Ox-LDL damaged the cells. But in the presence of the tested compounds, the cell survival rate increased. When the compounds 1 and 3 were 50 μM , the survival rate increased significantly ($p < 0.01$); at 100 μM , it increased to 85.9% and 89.2%, respectively. The results showed that the compounds improved the survival rate of HUVEC cells damaged by ox-LDL, but there was no significant difference between 50 μM and 100 μM .

Table 1
 H_2S releasing half-lives.

Compound	C_{max} of H_2S (μM)	$t_{1/2}$ (min)	Compound	C_{max} of H_2S (μM)	$t_{1/2}$ (min)
1	41.4	15.3	10	15.6	1.5
2	32.2	19.8	11	17.8	1.2
3	38.6	21.3	12	18.3	0.9
4	18.1	2.1	13	14.7	0.8
5	15.8	3.9	14	17.2	1.7
6	17.3	5.6	15	16.9	1.2
7	12.0	3.3	16	14.4	1.4
8	11.4	4.2	17	15.8	1.0
9	16.2	2.1	18	15.2	0.9

$T_{1/2}$: H_2S releasing half-lives when compounds at 60 μM .



Scheme 3. The structures and synthetic route of compounds 9–18.

Table 2
IC₅₀ values of all the compounds.

Compound	IC ₅₀ (μM)			
	H9c2	HUVEC	RAW264.7	W138
1	> 800	> 800	> 800	> 800
2	> 800	> 800	> 800	> 800
3	> 800	> 800	> 800	> 800
4	753.8 ± 5.6	683.1 ± 6.3	> 800	> 800
5	780.2 ± 3.7	713.7 ± 7.2	> 800	> 800
6	797.4 ± 4.5	755.2 ± 4.3	> 800	> 800
7	627.4 ± 5.1	562.3 ± 2.9	> 800	733.5 ± 4.7
8	675.2 ± 4.9	616.5 ± 6.4	> 800	763.6 ± 3.8
9	> 800	701.3 ± 3.9	> 800	> 800
10	> 800	691.8 ± 4.8	> 800	> 800
11	> 800	723.7 ± 6.5	> 800	> 800
12	726.4 ± 5.6	566.7 ± 5.2	> 800	> 800
13	694.5 ± 7.3	549.6 ± 6.3	> 800	780.7 ± 6.1
14	> 800	728.6 ± 5.7	> 800	> 800
15	> 800	772.56 ± 4.7	> 800	> 800
16	> 800	790.9 ± 4.9	> 800	> 800
17	771.1 ± 7.4	661.1 ± 8.2	> 800	> 800
18	746.6 ± 5.1	615.5 ± 7.4	> 800	779.8 ± 4.4

Compounds **9** and **14** also increased the survival rate significantly under the same condition ($p < 0.05$), but the effects are weaker than those of compounds **1** and **3**.

In order to observe the damage of HUVEC cells more intuitively, the cells were stained with Hoechst3342, PI and JC-1, and observed under fluorescence microscope. After hoechst3342 staining, the HUVEC nucleus showed weak blue fluorescence and complete fluorescence morphology; and the chromatin was uniformly distributed. In the model group, the HUVEC nucleus showed strong blue fluorescence, and some were pyknosis; the chromatin condensation and apoptotic bodies appeared. But in the presence of the compound, the nuclear pyknosis and apoptotic bodies significantly reduced. In Fig. 3, the late apoptosis and death cells were stained red by PI. Many cells in model group were stained red, while only a few cells were stained red in compound group. This indicates the tested compounds inhibited some injured cells, and compound **3** displayed better activity. After JC-1 staining, the mitochondria of most HUVEC showed red fluorescence, but the strong green fluorescence was observed in the HUVEC treated with Ox-LDL, indicating the membrane potential of mitochondria of HUVEC decreased (the fluorescence changed from red to green), which indicates Ox-LDL induced the HUVEC early apoptosis. In the presence of the tested compounds, the HUVEC showed weak red fluorescence, indicating only a few cells early apoptosis. The results showed the compounds obviously inhibited the apoptosis of HUVEC cells induced by Ox-LDL.

In order to further understand the process of the HUVEC apoptosis, the expression levels of three apoptosis-regulating genes were

measured. The anti-apoptosis gene bcl-2 and the pro-apoptotic gene bax are two important regulatory genes, which have opposite functions in the process of apoptosis regulation.²⁴ Caspase-3 is the one of key executive molecule in the process of apoptosis. As shown in the Fig. 4, the expression of bax and caspase-3 increased significantly and bcl-2 decreased significantly when the cells treated with Ox-LDL. However, after incubation with the tested compounds, the levels of both bax and caspase-3 in the cells treated with Ox-LDL down-regulated. In contrast, compound **1** at 50 μM was the most obvious ($p < 0.01$). Compounds **1** and **3** were 50 μM, the expression levels of bcl-2 in the cells up-regulated by 32.7 and 31.9%, respectively. This suggests that compounds **1** and **3** protected HUVEC cells from damage by affecting apoptotic proteins.

2.5. The effect of compounds on the formation of foam cells mediated by ox-LDL

Oxidized low density lipoprotein (Ox-LDL) is formed by oxidation of low density lipoprotein (LDL) in blood and blood vessels. Ox-LDL has strong affinity to scavenger receptors (such as CD36, SRA and LOX-1) on the surface of mononuclear macrophages; consequently it is quickly captured and swallowed by macrophages.²⁵ However, Ox-LDL is highly toxic to macrophages, which makes the macrophages to be foam cells by activating mononuclear macrophages rapid proliferation, aggregation and degeneration; the accumulation of these foam cells forms lipid plaques of atherosclerosis (As).²⁶ In addition, Ox-LDL can cause intracellular signal disorder and endothelial cell dysfunction by combining with LOX-1 in vascular endothelial cell. Ox-LDL can also promote vascular smooth muscle cells to continuously proliferate and migrate outward, and form plaque in the inner wall of blood vessel. The formation of foam cell is one of the key factors in the formation of atherosclerosis.²⁷ The formation of Ox-LDL is connected with the ROS level, so the compound as H₂S donors possibly influence foam cell formation.

In order to confirm this point, we chose Ox-LDL treated RAW264.7 cell model and evaluated the effect of compound on the formation of foam cells. Oil Red O stain, a well-established and classical method,²⁸ was used to examine foam cell formation in macrophages. The testing results show most of the macrophages had no red lipid droplets and the morphology was intact in the control group. Induced by Ox-LDL, the macrophages increased in size and many red lipid droplets were clearly observed in the cytoplasm, which were arranged in a ring shape on the inner side of the cell membrane, with a large lipid droplet in the cluster. But in the presence of compound **1** or **3**, the red lipid droplets in macrophages reduced in dose-dependent manner; and compounds **1** and **3** displayed stronger activity than the corresponding precursor nicotinic acid and clofibrate. When they were up to 50 μM, the red lipid droplets in macrophages were reduced more significantly (Fig. 5).

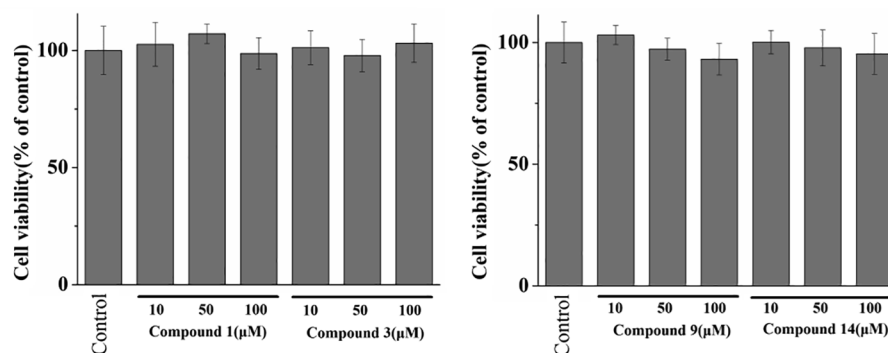


Fig. 1. Effects of the compounds on viability rate of HUVEC cell line. Each bar represents the mean ± SD of six independent experiments. There was no significant difference in the compounds group compared with the control group.

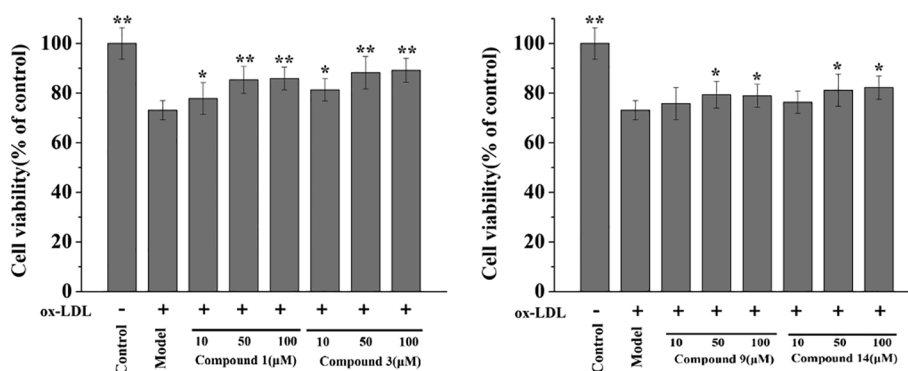


Fig. 2. Effect of the compounds on the viability rate of HUVEC cells damaged by ox-LDL. Data are presented as mean \pm SD (n = 6) from three independent experiments. *P < 0.05, ** P < 0.01, compared with model via one-way ANOVA.

2.6. The effect of compounds on intracellular lipid accumulation in RAW264.7 cells treated with ox-LDL

The compounds as H₂S donors displayed inhibitory effects against intracellular lipid accumulation in Ox-LDL-treated RAW264.7 cells. To further confirm this result, a cholesterol kit was used to detect total cholesterol and free cholesterol in cells, and the ratio of cholesterol ester to total cholesterol were calculated. The results show in Fig. 6, after the cells treated with Ox-LDL, the contents of total intracellular cholesterol (TC), free cholesterol (FC) and cholesterol ester (CE) increased. The value of CE/TC was higher than that in the control group (p < 0.01), and it exceeded 50%. However, in the presence of the compounds, the TC and FC content of cells was decreased (p < 0.05); moreover, the decreases reduced by the compounds were more significant than those caused by the corresponding precursors (p < 0.01). When compound 3 was 50 μM, the TC and FC contents were decreased

by 52.4% and 25.4%, respectively. Under the action of compound 1 and compound 3 (50 μM), the ratio of CE/TC was reduced by 32.4% and 30.9%, respectively. The results showed that compound 1 and compound 3 significantly inhibited lipid accumulation, and further inhibited the formation of foam cells.

2.7. The effect of compounds on ROS and MDA levels in RAW264.7 cells treated with ox-LDL

In the progression of atherosclerosis, the role of oxidative stress has been widely focused on.^{29,30} The ROS produced in oxidative stress is one of the important factors which forming Ox-LDL. The compounds released H₂S, and H₂S can react with ROS. Thus, the compounds can prevent the progression of atherosclerosis through attenuating oxidative stress. On the basis of this theory, the ROS and MDA levels RAW264.7 cells treated with Ox-LDL were measured. After the

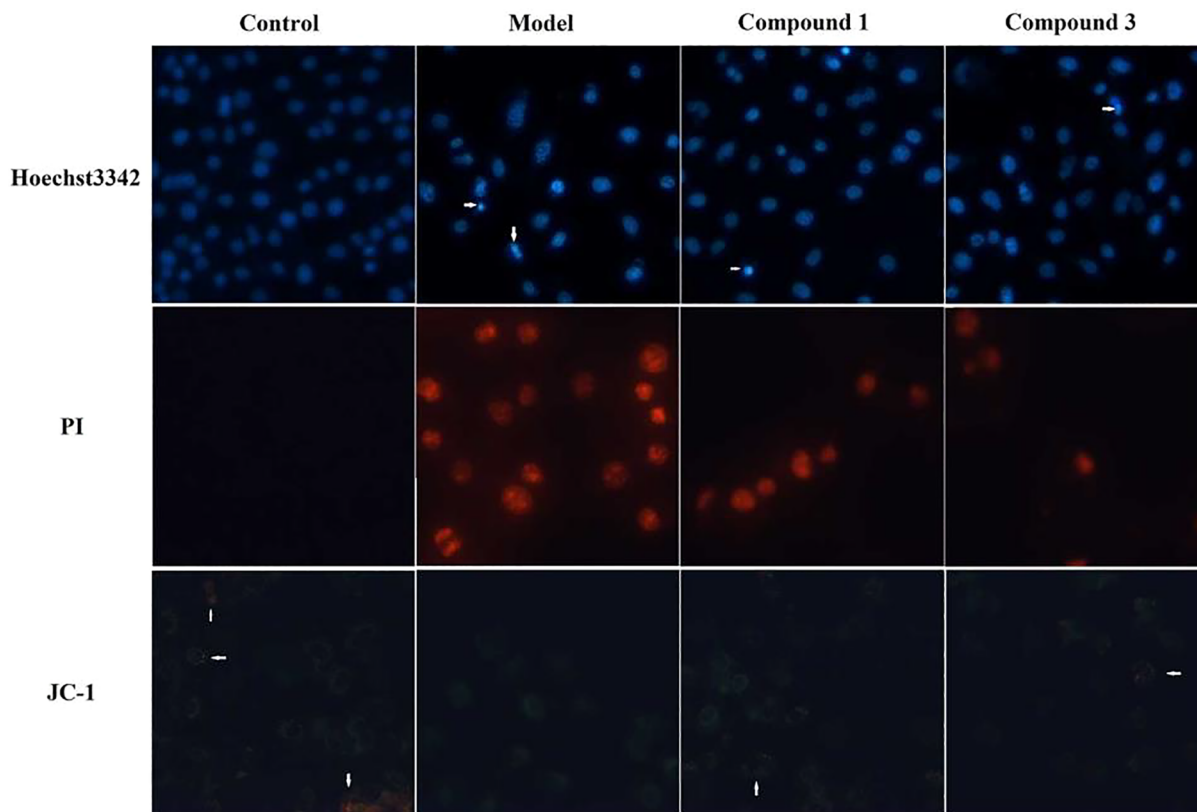


Fig. 3. After incubation, cells were stained with Hoechst33342, PI and JC-1, respectively, and the changes of nucleus and mitochondrial membrane potential of HUVEC cells were observed under the fluorescence microscope ($\times 200$).

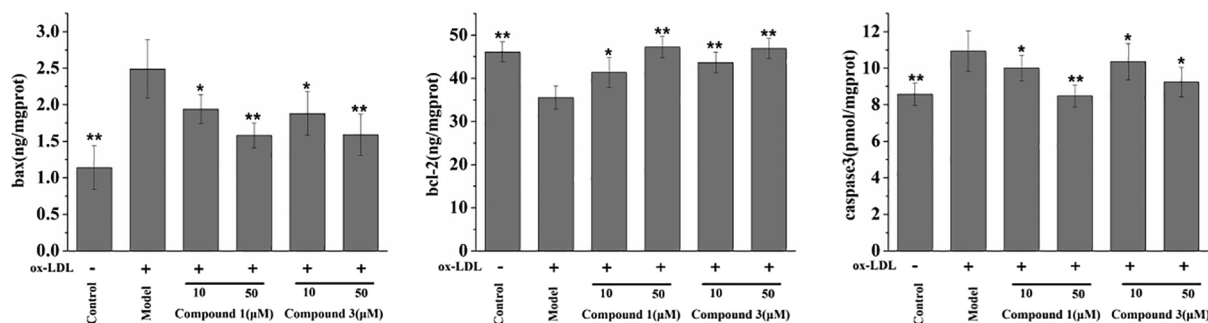


Fig. 4. The effect of compounds on the expression of bax, bcl-2 and caspase3 in HUVEC cells. Data are presented as mean \pm SD (n = 6) from three independent experiments. *P < 0.05, ** P < 0.01, compared with model via one-way ANOVA.

incubation, the cells were stained with DCFH-DA fluorescent probes; and the green fluorescence was observed (Fig. 7). The stronger the intensity of green fluorescence, the higher ROS level in cells. The testing results are shown in Fig. 8. In the model group which infected with Ox-LDL, the ROS and MDA were higher than (p < 0.01) the blank control and the SOD level was significantly lower (p < 0.01). However, in the presence of compound 1 or compound 3, the ROS and MDA levels were decreased compared with the model group, while SOD production increased. And when the concentration is 50 μ M, compound 1 and 3 increased the SOD levels by 48.3% and 45.4%, whereas MDA levels decreased by 47.0% and 41.0%. In addition, niacin and clofibrate did not display significant activity to ROS, MDA and SOD. These results further suggest that the effect of compound resulted from H₂S releasing.

2.8. Anti-inflammation of the compounds

Next, to evaluate whether compounds can reduce vascular inflammation, enzyme linked immunosorbent assay was carried out. As shown in Fig. 9, Ox-LDL significantly enhanced the TNF- α level (pro-inflammatory cytokine) in RAW264.7 cells, which increased by 175.2% compared with the control. The uptake of Ox-LDL by RAW264.7 cells induced foam cell formation, which accompanying with the presence of oxidative stress and severe inflammatory reactions. In the presence of the compounds, the level of TNF- α decreased significantly, and the level of IL-10 (anti-inflammatory cytokine) increased. Moreover, this effect was dose-dependent. Niacin and clofibrate also decreased TNF- α and increased IL-10. But their mechanism of action is different from

that of the compounds as H₂S donors. Niacin and clofibrate are anti-lipemic agents in clinic. They possibly inhibited the synthesis of VLDL and reduced intake of Ox-LDL by microphage, thereby showed anti-inflammatory effects. The compound not only released H₂S, but reduced Ox-LDL intake by microphage, so they displayed better activity than the niacin and clofibrate.

2.9. Effect of compounds on PI3K, Akt and NF- κ B expression in RAW 264.7 cells

During atherosclerosis, PI3K/Akt/NF- κ B pathway may be activated to promote the synthesis and secretion of vascular fibroblasts, smooth muscle cells, collagen and other components, and accelerate the process of arteriosclerosis. The increasing evidence indicates that PI3K/Akt/NF- κ B contributes to many features of atherosclerosis, including foam cell formation, vascular inflammation, VSMC proliferation, calcification, plaque development and disruption, and vascular cell apoptosis.³¹⁻³⁶ Therefore, the main protein expression of this signal pathway was examined in the RAW264.7 cells. The results show in Fig. 10, the expression levels of PI3K, Akt and NF- κ B in Ox-LDL-induced RAW264.7 cells significantly up-regulated (p < 0.01) compared with the control. But in the presence of compound 1 or 3, all the expression levels down-regulated (p < 0.01 or p < 0.05), and the higher the concentration, the more obvious the inhibition effect was (p < 0.01).

Therefore, in the progress of atherosclerosis, the compounds not only interfere with lipid metabolism, but also interfere with the expression of key proteins in PI3K/Akt/NF- κ B pathway, and then inhibit

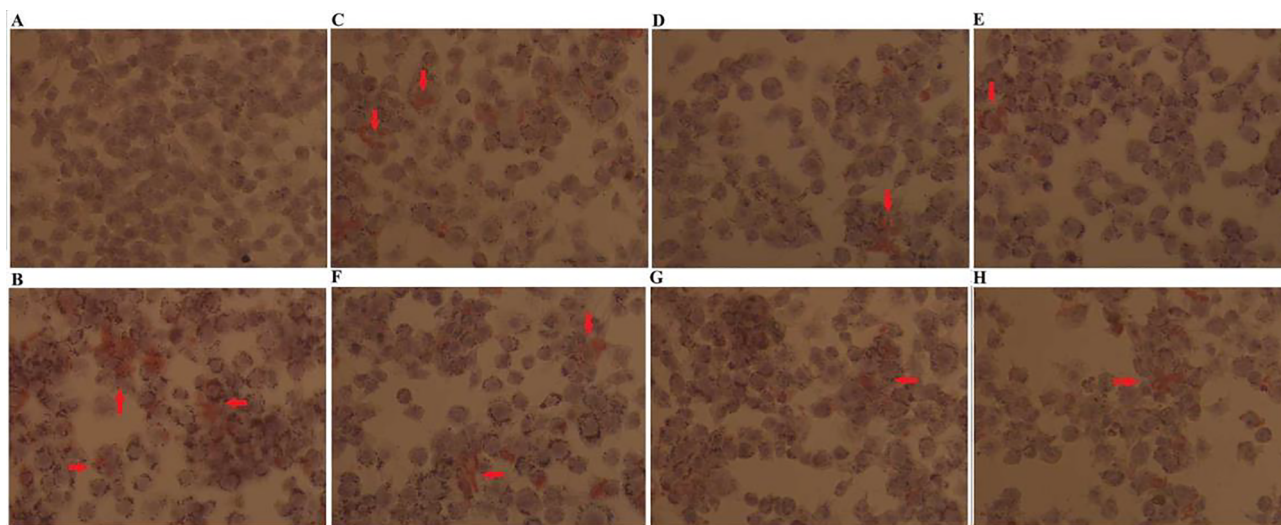


Fig. 5. After treated with the compound, the morphology of RAW264.7 cells were stained with Oil Red O and observed under the optical microscope (\times 200): A for control; B for Ox-LDL; C for Ox-LDL + nicotinic acid; D for Ox-LDL + compound 1 (10 μ M); E for Ox-LDL + compound 1 (50 μ M); F for Ox-LDL + clofibrate (10 μ M); G for Ox-LDL + compound 3 (10 μ M); H for Ox-LDL + compound 3 (50 μ M).

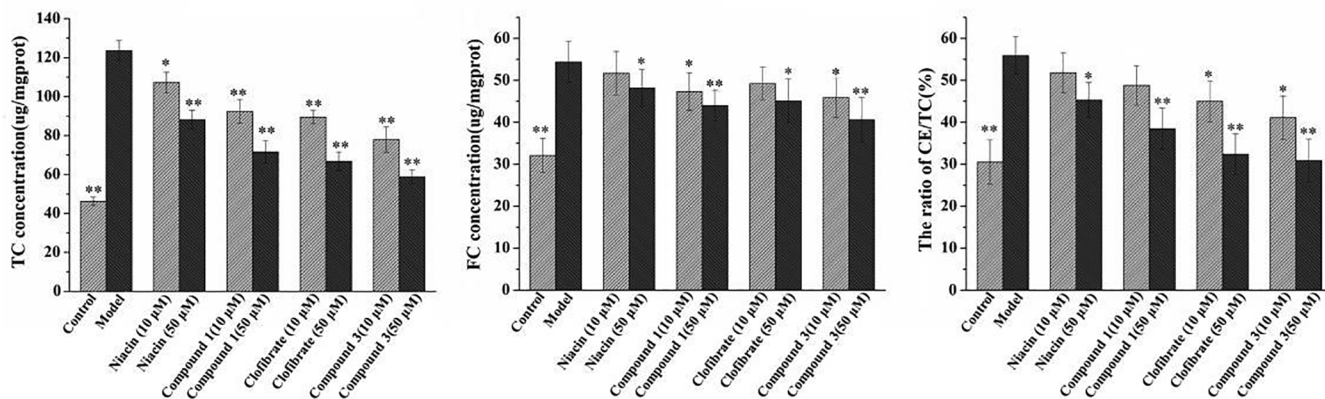


Fig. 6. Total intracellular cholesterol (TC) and free cholesterol (FC) contents in the Ox-LDL-treated RAW264.7 cells in the presence (absence) of the compound. The mass of cholesterol ester (CE) was calculated by subtracting FC from TC. Data are presented as mean \pm SD (n = 6) from three independent experiments. *P < 0.05, ** P < 0.01, compared with model via one-way ANOVA.

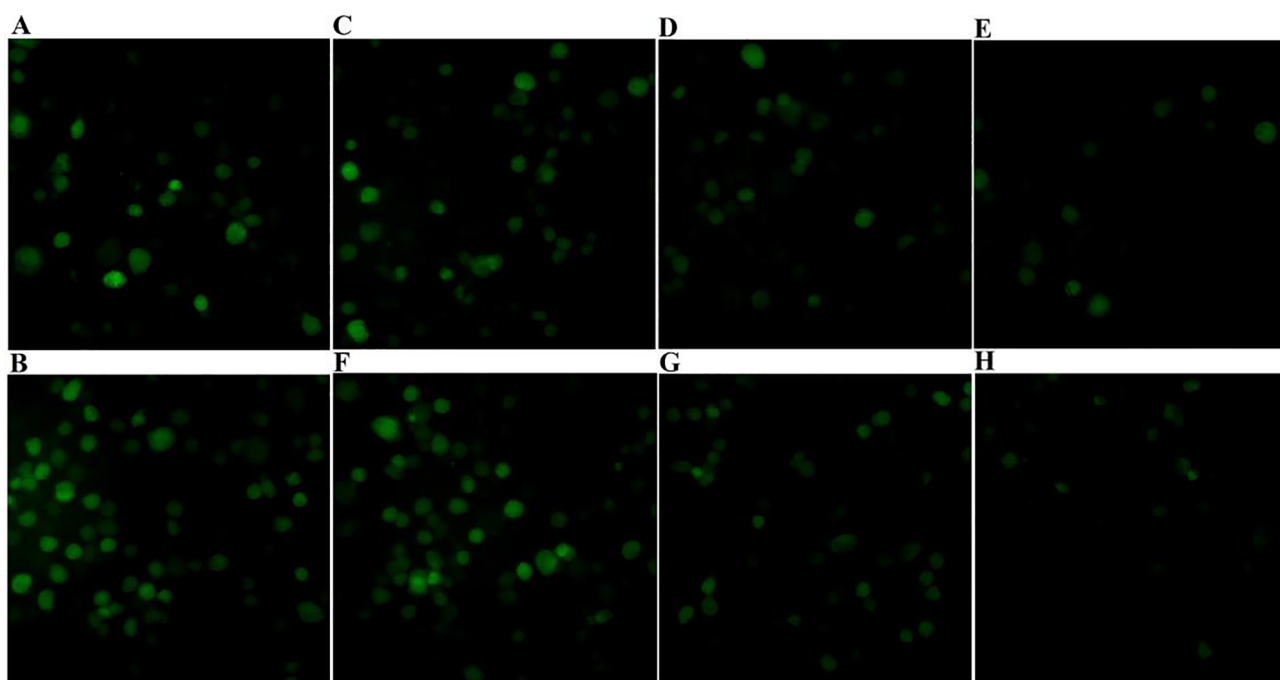


Fig. 7. The effect of compounds on the fluorescence intensity of ROS in the cells ($\times 200$). A for the control; B for Ox-LDL (100 μ g/ml); C for Ox-LDL + nicotinic acid (10 μ M); D and E for Ox-LDL + compound 1 (10 and 50 μ M); F for Ox-LDL + clofibrate (10 μ M); G and H for Ox-LDL + compound 3 (10 and 50 μ M).

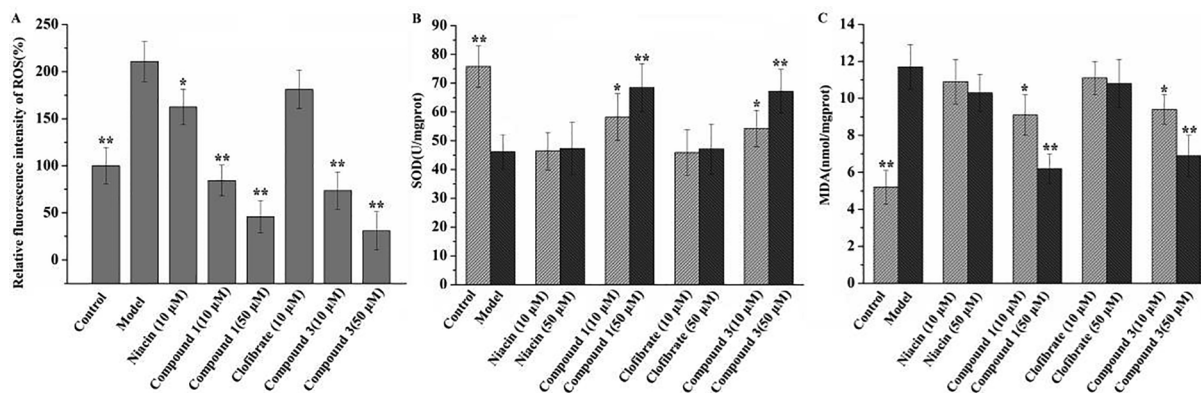


Fig. 8. Effect of the compound on ROS, SOD and MDA levels in RAW264.7 cells treated with ox-LDL; Data are presented as mean \pm SD (n = 6) from three independent experiments. *P < 0.05, ** P < 0.01, compared with model via one-way ANOVA.

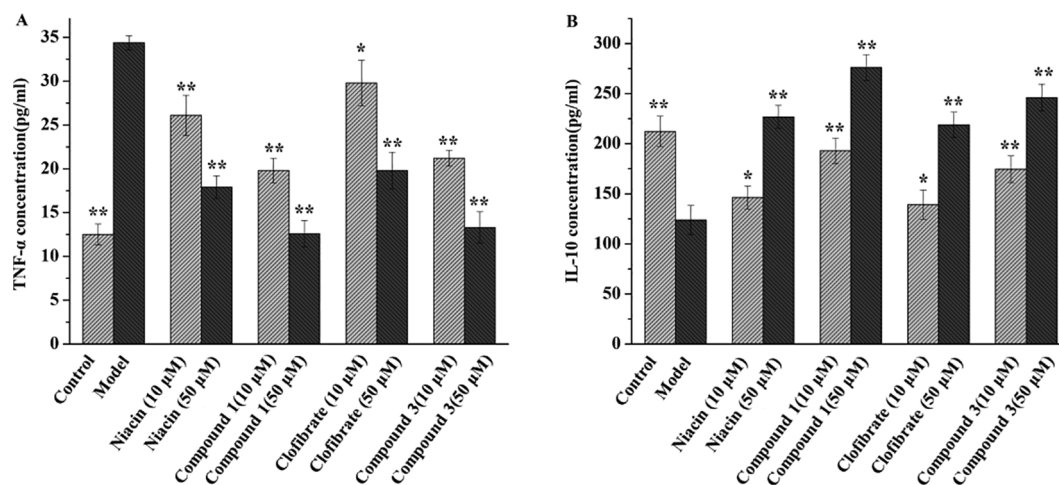


Fig. 9. Effect of the compound on ox-LDL induced inflammatory reaction, A for TNF- α level; B for IL-10 level. Data are presented as mean \pm SD (n = 6) from three independent experiments. *P < 0.05, ** P < 0.01, compared with model via one-way ANOVA.

the process of arteriosclerosis.

3. Conclusions

Based on the pro-drug principle, structures of a series of H₂S donors modified with nicotinic acid or chlorfibrate were synthesized. They can effectively release H₂S. All the compounds showed no significant cytotoxicity to four normal cell lines (IC₅₀ > 500 μ M). In the activity experiment, three compounds could increase the survival rate of HUVEC cells after ox-LDL damage. The protective effects of compounds 1 and 3 were more obvious, this may have something to do with their ability to release H₂S more persistently. They can reduce the expression of apoptosis-related protein bax and caspase 3, increase the expression of protein bcl-2, reduce apoptosis, and inhibit HUVEC cells from ox-LDL damage. In addition, compounds 1 and 3 inhibited the formation of foam cells. This may be achieved by reducing lipids in foam cells, reducing inflammation and anti-oxidation. This may be due to the decomposition of the compound into lipid lowering drugs and H₂S donors under the action of esterase in the biological environment, thus showing synergistic effects. In addition, nicotinic acid and chlorfibrate did not show obvious antioxidant effect, but compounds 1 and 3 could significantly reduce ROS and MDA, and increase the expression of SOD. This may be that H₂S play a role in reducing free radicals. The results showed that the compounds not only inhibited the apoptosis of HUVEC

cells, but also inhibited the formation of foam cells by regulating lipid metabolism, anti-inflammation and decreasing lipid peroxidation.

All these suggest the compounds can inhibit several factors of atherosclerosis, therefore, possibly there is a kind multi-target anti-atherosclerosis candidates and has a potential application in clinic. However, what are their pharmacokinetic properties and what kind patient will be suitable for them? To answer these questions, it needs lots of work to do.

4. Experimental

4.1. Reagents and antibodies

The H9c2, W138, HUVEC and RAW264.7 macrophage cell line was purchased from the cell resources Center for Shanghai Life Science Institute of Chinese Academy of Sciences (China). Reagents for cell culture were bought from Gibco (Grand Island, USA). All ELISA and content assay kit were purchased from Beijing Solarbio Science & Technology (Beijing, China). Oil red O were purchased from Sigma (St. Louis, MO, USA). Ox-LDL were purchased from Yiyuan Biotechnologies (Guangzhou, China). Rabbit anti-mouse monoclonal antibodies to PI3K, Akt, NF- κ b and CSE were purchased from Cell Signaling Technology, Inc. (Boston, America). Horseradish peroxidase-labelled goat anti-rabbit IgG was purchased from Affinity Biosciences (Changzhou,

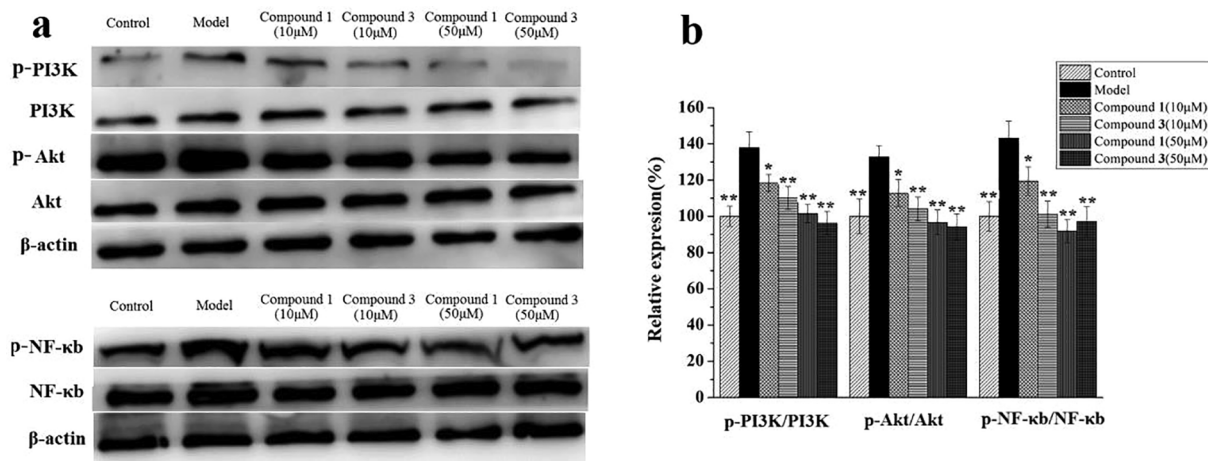


Fig. 10. Effect of compounds on PI3K, Akt and NF- κ b protein expression in macrophages. Data are presented as mean \pm SD (n = 3) from three independent experiments. *P < 0.05, ** P < 0.01, compared with model via one-way ANOVA.

China).

4.2. Preparation of all the compounds

All reactions were carried out under nitrogen atmosphere and room temperature. Solvents for reactions were degassed and distilled from the proper drying agents. DCM and THF were used as solvents for reactions. All reactions were followed by TLC, carried out on silica gel 254 plates with fluorescent indicator and the plates were visualized with UV light (254 nm). Solutions were dried over Na_2SO_4 and concentrated with rotary evaporator at low pressure. All products can be separated by column chromatography with different ratios of chloroform and methanol.

IR spectra were recorded on a Nicolet NEXUS 360 spectrophotometer, and NMR spectra on a BrukerAM-400 MHz spectrometer. A Lambda 25 UV-Visible spectrophotometer and a Maxis-4G TOF Mass spectrometer (ESI) were used.

Compound 1. A solution of 1,3-propanediol (3.04 g, 40 mmol) in tetrahydrofuran (150 mL) and EDC-HCl (1.84 g, 9.6 mmol), DMAP (0.39 g, 3.2 mmol) was stirred at room temperature and to it nicotinic acid (1.0 g, 8 mmol) was added in several portions. Upon completion of the reaction, the solution was washed with distilled water once (100 mL). Extraction of the ester was effected with chloroform ($\times 3$). The combined chloroform extracts were dried on anhydrous Na_2SO_4 , decanted and evaporated. Purification was obtained by chromatography on flash silica (chloroform/methanol, 20/1). Compound **A1** (0.89 g) was obtained as a yellow oil. Yield: 64%. IR(KBr, cm^{-1}): 2931(s), 1727(vs), 1420(m), 1286(s), 1176(m), 1025(m), 732(m). ^1H NMR(400 MHz, CDCl_3 -d) δ 9.21(s, 1H), 8.77(s, 1H), 8.30(d, $J = 8.0$ Hz, 1H), 7.49–7.35(m, 1H), 4.53(t, $J = 6.2$ Hz, 2H), 3.81(t, $J = 6.1$ Hz, 2H), 2.81(s, 1H), 2.04(p, $J = 6.1$ Hz, 2H). ^{13}C NMR(101 MHz, CDCl_3 -d) δ 165.4, 153.2, 150.7, 137.2, 126.2, 123.4, 62.4, 58.8, 31.7. ESI-HRMS (m/z): Calcd. for $\text{C}_9\text{H}_{11}\text{NO}_3$ $[\text{M} + \text{H}]^+$: 182.0829; found 182.0817.

A1 (200 mg, 1.1 mmol) was dissolved in 100 mL of dry CH_2Cl_2 , then (\pm)- α -Lipoic acid (227 mg, 1.1 mmol), the catalysts EDC-HCl (253 mg, 1.3 mmol) and DMAP (49 mg, 0.4 mmol) was added. The reaction mixture was stirred for 12 h at room temperature. The solvent was removed in vacuo, the residue was extracted with a small amount of DCM, and the extract was subjected to silica gel column chromatography (chloroform/methanol 40/1). Compound **1** (267 mg) as a yellow oil was obtained; Yield: 66%. IR (KBr, cm^{-1}): 2931(s), 1727(vs), 1591(s), 1420(m), 1284(m), 1176(m), 1112(m), 741(m). ^1H NMR (400 MHz, CDCl_3 -d) δ 9.24(s, 1H), 8.80(d, $J = 4.5$ Hz, 1H), 8.32(d, $J = 7.9$ Hz, 1H), 7.43(dd, $J = 7.8, 4.9$ Hz, 1H), 4.46(t, $J = 6.3$ Hz, 2H), 4.25(t, $J = 6.2$ Hz, 2H), 3.57(p, $J = 6.5$ Hz, 1H), 3.23–3.09(m, 2H), 2.53–2.40(m, 1H), 2.33(t, $J = 7.4$ Hz, 2H), 2.21–2.09(m, 2H), 1.92(dt, $J = 12.9, 6.9$ Hz, 1H), 1.67(dt, $J = 12.8, 6.6$ Hz, 4H), 1.48(dt, $J = 10.3, 5.9$ Hz, 1H), 1.25(s, 1H). ^{13}C NMR(101 MHz, CDCl_3 -d) δ 172.3, 164.1, 152.4, 149.8, 136.0, 124.9, 122.3, 61.0, 59.8, 55.3, 39.2, 37.4, 33.5, 32.9, 27.7, 27.0, 23.6. ESI-HRMS(m/z): Calcd. for $\text{C}_{17}\text{H}_{23}\text{NO}_4\text{S}_2$ $[\text{M} + \text{Na}]^+$: 392.0980; found 392.0966.

The procedure and workup of compounds 2–3 were similar to the process of compound 1 and the procedure and workup of compounds **A2**–**A3** were similar to the process of compound **A1**.

Compound 2 Yield: 58%. IR(KBr, cm^{-1}): 2918(s), 1727(vs), 1595(s), 1360(m), 1181(m), 1101(m), 780(m). ^1H NMR(400 MHz, CDCl_3 -d) δ 8.73(s, 1H), 8.50(s, 1H), 4.45(t, $J = 6.4$ Hz, 2H), 4.16(t, $J = 6.1$ Hz, 2H), 3.50(dt, $J = 14.3, 6.4$ Hz, 1H), 3.15–3.00(m, 2H), 2.45(s, 3H), 2.39(dd, $J = 12.4, 5.9$ Hz, 1H), 2.26(t, $J = 7.4$ Hz, 2H), 2.08(s, 2H), 1.85(dt, $J = 12.8, 6.9$ Hz, 1H), 1.60(dt, $J = 15.0, 7.8$ Hz, 4H), 1.40(dt, $J = 15.7, 7.7$ Hz, 2H). ^{13}C NMR(101 MHz, CDCl_3 -d) δ 172.2, 161.4, 146.3, 146.2, 144.1, 134.3, 62.3, 59.5, 55.3, 39.2, 37.4, 33.5, 32.9, 27.7, 26.9, 23.6, 13.7. ESI-HRMS(m/z): Calcd. for $\text{C}_{17}\text{H}_{24}\text{N}_2\text{O}_5\text{S}_2$ $[\text{M} + \text{Na}]^+$: 423.1030; found 423.1024.

Compound A2 Yield: 58%. IR(KBr, cm^{-1}): 2946(s), 1727(vs), 1469(m), 1313(m), 1239(m), 1061(m), 747(m). ^1H NMR(400 MHz,

CDCl_3 -d) δ 8.81(s, 1H), 8.56(s, 1H), 4.60(t, $J = 6.3$ Hz, 2H), 3.81(t, $J = 5.8$ Hz, 2H), 2.53(s, 3H), 2.25(s, 1H), 2.06(q, $J = 6.1$ Hz, 2H). ^{13}C NMR(101 MHz, CDCl_3 -d) δ 162.6, 147.3, 147.2, 145.2, 135.3, 64.0, 59.1, 31.4, 14.7; ESI-HRMS(m/z): Calcd. for $\text{C}_9\text{H}_{12}\text{N}_2\text{O}_4$ $[\text{M} + \text{Na}]^+$: 235.0682; found 235.0695.

Compound 3 Yield: 62%. IR(KBr, cm^{-1}): 2939(vs), 2365(s), 1735(vs), 1489(vs), 1239(m), 1174(s), 1142(m), 829(m), 669(m). ^1H NMR(400 MHz, CDCl_3 -d) δ 7.12(d, $J = 8.9$ Hz, 2H), 6.70(d, $J = 8.9$ Hz, 2H), 4.16(t, $J = 6.3$ Hz, 2H), 3.98(t, $J = 6.2$ Hz, 2H), 3.54–3.45(m, 1H), 3.16–2.99(m, 2H), 2.39(dd, $J = 12.4, 6.0$ Hz, 1H), 2.24(t, $J = 7.4$ Hz, 2H), 1.86(dt, $J = 13.8, 6.5$ Hz, 3H), 1.65–1.55(m, 4H), 1.52(s, 6H), 1.38(s, 2H). ^{13}C NMR(101 MHz, CDCl_3 -d) δ 172.8, 172.2, 152.9, 128.1, 126.2, 119.3, 78.4, 61.0, 59.5, 55.2, 39.2, 37.4, 33.5, 32.90, 27.7, 26.8, 24.3, 23.6; ESI-HRMS(m/z): Calcd. for $\text{C}_{21}\text{H}_{29}\text{ClO}_5\text{S}_2$ $[\text{M} + \text{Na}]^+$: 483.1050; found 483.1043.

Compound A3 Yield: 62%. IR(KBr, cm^{-1}): 2931(vs), 1735(vs), 1526(vs), 1284(m), 1185(s), 1142(m), 781(m). ^1H NMR(400 MHz, CDCl_3 -d) δ 7.20(d, $J = 8.9$ Hz, 2H), 6.78(d, $J = 8.9$ Hz, 2H), 4.31(t, $J = 6.2$ Hz, 2H), 3.59(t, $J = 6.0$ Hz, 2H), 2.04(s, 1H), 1.85(p, $J = 6.1$ Hz, 2H), 1.58(s, 6H). ^{13}C NMR(101 MHz, CDCl_3 -d) δ 174.2, 153.9, 129.1, 127.3, 120.4, 79.5, 62.6, 59.0, 31.4, 25.3; ESI-HRMS(m/z): Calcd. for $\text{C}_{13}\text{H}_{17}\text{ClO}_4$ $[\text{M} + \text{H}]^+$: 273.0875; found 273.0894.

Compound 4 A solution of nicotinic acid (500 mg, 4.0 mmol) in THF (100 mL) and EDC-HCl(920 mg, 4.8 mmol), DMAP(146 mg, 1.2 mmol) was stirred at room temperature and to it 4-hydroxythiobenzamide (612 mg, 4.0 mmol) was added. The reaction mixture was stirred for 12 h at room temperature. The solvent was removed in vacuo, the residue was extracted with a small amount of DCM, and the extract was subjected to silica gel column chromatography (chloroform/methanol, 30/1). Compound **4** (450 mg) as a yellow oil was obtained; Yield: 45%. IR(KBr, cm^{-1}): 3330(s), 1728(s), 1643(s), 1446(vs), 1387(m), 1271(m), 885(m), 627(m). ^1H NMR (400 MHz, CDCl_3 -d) δ 9.41(s, 1H), 8.87(d, $J = 6.0$ Hz, 1H), 8.49(d, $J = 7.7$ Hz, 1H), 7.75(d, $J = 10.6$ Hz, 2H), 7.54–7.49(m, 1H), 7.43(s, 1H), 7.40(s, 1H), 6.91(s, 2H). ^{13}C NMR(101 MHz, CDCl_3 -d) δ 189.6, 171.4, 158.7, 157.2, 146.1, 143.7, 132.4, 130.8, 127.4, 124.5. ESI-HRMS(m/z): Calcd. for $\text{C}_{13}\text{H}_{10}\text{N}_2\text{O}_2\text{S}$ $[\text{M} + \text{Na}]^+$: 281.0382; found 281.0361.

The procedure and workup of compounds 5–8 were similar to the process of compound 4

Compound 5 Yield: 59%. IR(KBr, cm^{-1}): 3352(s), 1689(s), 1524(s), 1504(vs), 1237(m), 1162(m), 1054(s), 782(m). ^1H NMR(400 MHz, CDCl_3 -d) δ 4.45(d, $J = 17.1$ Hz, 2H), 2.93(s, 1H), 2.62(t, $J = 11.8$ Hz, 1H), 1.85–1.44(m, 4H), 1.18(s, 1H), 0.90(d, $J = 6.7$ Hz, 3H). ^{13}C NMR (101 MHz, CDCl_3 -d) δ 211.7, 196.3, 54.6, 48.7, 31.2, 17.3. ESI-HRMS (m/z): Calcd. for $\text{C}_{11}\text{H}_{12}\text{O}_4\text{NS}_2$ $[\text{M} + \text{H}]^+$: 290.0586; found 290.0599.

Compound 6 Yield: 54%. IR(KBr, cm^{-1}): 3324(s), 1757(vs), 1600(vs), 1489(vs), 1237(m), 1168(vs), 1114(vs), 902(m), 827(m). ^1H NMR(400 MHz, CDCl_3 -d) δ 7.68(d, $J = 8.7$ Hz, 2H), 7.40(s, 1H), 7.27(s, 1H), 7.25(d, $J = 8.7$ Hz, 2H), 7.16(d, $J = 8.7$ Hz, 2H), 6.90(s, $J = 8.9$ Hz, 2H), 1.74(s, 6H). ^{13}C NMR(101 MHz, CDCl_3 -d) δ 186.4, 172.6, 157.4, 143.5, 132.8, 129.6, 127.3, 122.6, 81.4, 26.3. ESI-HRMS (m/z): Calcd. for $\text{C}_{17}\text{H}_{16}\text{ClNO}_3\text{S}$ $[\text{M} + \text{H}]^+$: 350.0632; found 350.0618.

Compound 7 Yield: 51%. IR(KBr, cm^{-1}): 1759(s), 1501(m), 1487(vs), 1237(s), 1126(m), 1016(m), 827(m). ^1H NMR (400 MHz, CDCl_3 -d) δ 9.42(s, 1H), 8.90(d, $J = 6.0$ Hz, 1H), 8.50(d, $J = 7.7$ Hz, 1H), 7.77(d, $J = 10.6$ Hz, 2H), 7.58–7.51(m, 1H), 7.44(s, 1H), 7.41(s, 1H), 7.39(s, 1H). ^{13}C NMR (101 MHz, CDCl_3 -d) δ 192.6, 182.5, 164.7, 154.3, 152.3, 150.5, 139.1, 137.4, 128.9, 126.3, 125.7, 122.4, 115.7. ESI-HRMS(m/z): Calcd. for $\text{C}_{15}\text{H}_9\text{NO}_2\text{S}_3$ $[\text{M} + \text{H}]^+$: 331.9889; found 331.9874.

Compound 8 Yield: 49%. IR(KBr, cm^{-1}): 1759(s), 1599(m), 1489(vs), 1168(s), 1110(s), 1026(m), 896(m), 827(m). ^1H NMR (400 MHz, CDCl_3 -d) δ 7.68(d, $J = 8.7$ Hz, 2H), 7.40(s, 1H), 7.27(s, 1H), 7.25(s, 1H), 7.16(d, $J = 8.7$ Hz, 2H), 6.90(d, $J = 8.9$ Hz, 2H), 1.75(s, 6H). ^{13}C NMR(101 MHz, CDCl_3 -d) δ 192.8, 177.1, 171.8, 155.3, 152.2, 134.8, 131.4, 128.9, 126.3, 122.1, 115.7, 89.5, 24.8. ESI-HRMS(m/z):

Calcd. for $C_{19}H_{15}ClO_3S_3$ [M+H]⁺: 422.9969; found 422.9950.

Compound **9** A solution of ethanolamine (2.44 g, 40 mmol) in tetrahydrofuran (200 mL) and EDC·HCl (1.84 g, 9.6 mmol), HOBT (1.08 g, 8.0 mmol) was stirred at room temperature and to it nicotinic acid (1.0 g, 8.0 mmol) was added in several portions. Upon completion of the reaction, the solution was washed with distilled water once (100 mL). Extraction of the ester was effected with chloroform (×3). The combined chloroform extracts were dried on anhydrous Na_2SO_4 , decanted and evaporated. Purification was obtained by chromatography on flash silica (chloroform/methanol 20/1). Compound **A₄** (0.76 g) was obtained as a yellow oil. Yield: 59%. IR (KBr, cm^{-1}): 3330(s), 2924(s), 1541(vs), 1165(m), 1014(m), 736(m). ¹H NMR (400 MHz, $CDCl_3$ -d) δ 9.01(s, 1H), 8.65(s, 1H), 8.14(d, $J = 6.6$ Hz, 1H), 7.49(s, 1H), 7.36(s, 1H), 3.92(s, 1H), 3.83(s, 2H), 3.62(s, 2H). ¹³C NMR (101 MHz, $CDCl_3$ -d) δ 166.3, 151.8, 147.7, 135.6, 130.2, 123.7, 61.4, 42.8. ESI-HRMS(m/z): Calcd. for $C_8H_{10}N_2O_2$ [M+H]⁺: 167.0732; found 167.0821.

A₄ (100 mg, 0.6 mmol) was combined with 2-chloro-4-nitrophenyl isothiocyanate (129 mg, 0.6 mmol) in anhydrous THF (30 mL) at 0 °C, followed by the addition of DBU (106 mg, 0.7 mmol). The resultant mixture was stirred at 0 °C for 20 min, after which the ice bath was removed, and the reaction mixture was stirred at room temperature until the completion of the reaction indicated by TLC. The crude product was purified by column chromatography (chloroform/methanol, 30/1). Compound **9** (157 mg) as a yellow oil was obtained. Yield: 69%. IR (KBr, cm^{-1}): 3330(s), 2924(s), 1649(s), 1513(vs), 1340(vs), 1196(m), 894(m), 736(m). ¹H NMR (400 MHz, $CDCl_3$ -d) δ 9.25(s, 1H), 8.75(s, 1H), 8.55(s, 1H), 8.31(s, 1H), 8.22(d, $J = 7.8$ Hz, 1H), 8.16(d, $J = 11.6$ Hz, 1H), 7.52(s, 1H), 7.26(s, 2H), 4.87(t, $J = 5.1$ Hz, 2H), 3.96(d, $J = 5.2$ Hz, 2H). ¹³C NMR (101 MHz, $CDCl_3$ -d) δ 191.2, 171.3, 166.9, 154.1, 151.6, 139.2, 133.5, 132.3, 131.6, 129.1, 115.8, 69.4, 43.2. ESI-HRMS(m/z): Calcd. for $C_{15}H_{13}ClN_4O_4S$ [M+Na]⁺: 403.0260; found 403.0244.

The procedure and workup of compounds 10–18 were similar to the process of compound **9** and the procedure and workup of compound **A₅** were similar to the process of compound **A₄**.

Compound **10** Yield: 74%. IR (KBr, cm^{-1}): 3330(s), 2931(s), 1593(s), 1513(vs), 1327 (vs), 1154(m), 736(m). ¹H NMR (400 MHz, $CDCl_3$ -d) δ 9.27(s, 1H), 8.76(s, 1H), 8.55(s, 1H), 8.31(s, 1H), 8.22(d, $J = 7.9$ Hz, 1H), 8.16(d, $J = 11.5$ Hz, 1H), 7.52(s, 1H), 7.26(s, 2H), 4.88(t, $J = 5.1$ Hz, 2H), 3.98(d, $J = 5.2$ Hz, 2H). ¹³C NMR (101 MHz, $CDCl_3$ -d) δ 190.5, 170.2, 168.4, 155.6, 152.3, 138.1, 135.2, 133.6, 132.9, 128.6, 115.2, 71.8, 41.4. ESI-HRMS(m/z): Calcd. for $C_{15}H_{14}FN_3O_2S$ [M+Na]⁺: 342.0693; found 342.0688.

Compound **11** Yield: 76%. IR (KBr, cm^{-1}): 3331(s), 2957(s), 1649(s), 1513(vs), 1340 (vs), 1181(m), 771(m). ¹H NMR (400 MHz, $CDCl_3$ -d) δ 8.54(s, 1H), 7.77(s, 1H), 7.35(s, 1H), 7.22(d, $J = 6.7$ Hz, 2H), 7.19(s, 2H), 7.11–7.06(m, 2H), 6.69(t, $J = 7.4$ Hz, 1H), 6.62(d, $J = 7.6$ Hz, 1H), 3.87–3.69(m, 2H), 3.55(s, 2H). ¹³C NMR (101 MHz, $CDCl_3$ -d) δ 190.8, 173.2, 158.4, 154.6, 140.1, 136.9, 136.2, 133.6, 132.9, 128.5, 125.6, 70.6, 42.3. ESI-HRMS(m/z): Calcd. for $C_{15}H_{15}N_3O_2S$ [M+Na]⁺: 324.0796; found 324.0783.

Compound **12** Yield: 68%. IR (KBr, cm^{-1}): 3330(s), 2924(s), 1652(s), 1541(vs), 1340 (vs), 1096(m), 689(m). ¹H NMR (400 MHz, $CDCl_3$ -d) δ 9.13(s, 1H), 8.86(s, 1H), 8.73(s, 1H), 8.19(s, 1H), 7.58–7.47(m, 2H), 7.25(d, $J = 8.5$ Hz, 1H), 6.92(d, $J = 8.4$ Hz, 1H), 6.78(d, $J = 8.7$ Hz, 1H), 4.62(s, 2H), 3.75(s, 2H), 2.25(s, 3H). ¹³C NMR (101 MHz, $CDCl_3$ -d) δ 190.8, 169.4, 160.7, 155.4, 152.1, 137.6, 136.6, 134.09, 132.7, 129.6, 128.4, 71.6, 61.4, 23.4. ESI-HRMS(m/z): Calcd. for $C_{16}H_{17}N_3O_2S$ [M+Na]⁺: 338.0943; found 338.0939.

Compound **13** Yield: 74%. IR (KBr, cm^{-1}): 3354(s), 2931(s), 1651(s), 1543(vs), 1343 (vs), 1154(m), 736(m). ¹H NMR (400 MHz, $CDCl_3$ -d) δ 10.99(d, $J = 24.6$ Hz, 1H), 9.02(d, $J = 13.5$ Hz, 1H), 8.86(s, 1H), 8.72(d, $J = 4.0$ Hz, 1H), 8.19(dd, $J = 14.2$ Hz, 1H), 7.55–7.46(m, 2H), 7.24(d, $J = 8.5$ Hz, 1H), 6.92(d, $J = 8.4$ Hz, 1H), 6.71(d, $J = 8.5$ Hz, 1H), 4.62(d, $J = 21.3$ Hz, 2H), 3.74(s, 2H), 3.36(s, 3H). ¹³C NMR

(101 MHz, $CDCl_3$ -d) δ 191.7, 170.2, 161.3, 157.2, 153.6, 140.2, 136.0, 134.9, 130.1, 128.6, 118.9, 72.1, 60.3, 43.54. ESI-HRMS(m/z): Calcd. for $C_{16}H_{17}N_3O_3S$ [M+H]⁺: 332.1081; found 332.1069.

Compound **14** Yield: 67%. IR (KBr, cm^{-1}): 3330(s), 2931(s), 1664(m), 1513(vs), 1489(vs), 1340(vs), 1183(s), 829(m), 736(m). ¹H NMR (400 MHz, $CDCl_3$ -d) δ 8.53(s, 1H), 8.14(s, 1H), 7.26(s, 2H), 7.20(s, 2H), 6.97(s, 1H), 6.82(s, 2H), 4.72(t, $J = 5.1$ Hz, 2H), 3.86–3.71(m, 2H), 1.49(s, 6H). ¹³C NMR (101 MHz, $CDCl_3$ -d) δ 186.1, 173.8, 151.5, 142.6, 138.2, 128.2, 127.6, 125.7, 123.9, 122.1, 121.3, 80.8, 69.3, 37.1, 23.9. ESI-HRMS(m/z): Calcd. for $C_{19}H_{19}Cl_2N_3O_5S$ [M+Na]⁺: 494.0413; found 494.0422.

Compound **A₅** Yield: 67%. IR (KBr, cm^{-1}): 3328(s), 2963(s), 1513(vs), 1368(s), 1153 (s), 896(m), 736(m). ¹H NMR (400 MHz, $CDCl_3$ -d) δ 7.24(d, $J = 8.8$ Hz, 2H), 6.87(d, $J = 8.8$ Hz, 2H), 3.73(d, $J = 10.1$ Hz, 2H), 3.47(q, $J = 5.5$ Hz, 2H), 2.66(s, 1H), 2.17(s, 1H), 1.49(s, 6H). ¹³C NMR (101 MHz, $CDCl_3$ -d) δ 175.7, 152.7, 129.2, 128.6, 122.7, 81.8, 62.1, 42.2, 24.9. ESI-HRMS(m/z): Calcd. for $C_{12}H_{16}ClNO_3$ [M+H]⁺: 258.0876; found 258.0897.

Compound **15** Yield: 76%. IR (KBr, cm^{-1}): 3244(s), 2965(s), 1666(vs), 1487(vs), 1340(m), 1060(s), 941(m), 732(m). ¹H NMR (400 MHz, Chloroform-d) δ 8.75(s, 1H), 7.39(s, 1H), 7.13(d, $J = 7.6$ Hz, 2H), 7.04(s, 1H), 6.88(s, 1H), 6.77(t, $J = 8.7$ Hz, 2H), 6.71(s, 1H), 6.59–6.50(m, 1H), 4.58(d, $J = 15.9$ Hz, 2H), 3.62(q, $J = 5.5$ Hz, 2H), 1.39(d, $J = 12.3$ Hz, 6H). ¹³C NMR (101 MHz, $CDCl_3$ -d) δ 188.3, 176.4, 164.5, 152.6, 133.9, 129.9, 126.5, 121.4, 117.2, 88.6, 69.7, 39.3, 24.2. ESI-HRMS(m/z): Calcd. for $C_{19}H_{20}ClFN_2O_3S$ [M+H]⁺: 411.0967; found 411.0945.

Compound **16** Yield: 71%. IR (KBr, cm^{-1}): 3224(s), 2965(s), 1666(vs), 1593(m), 1487(vs), 1397(s), 1261(s), 1153(s), 1092(s), 963(m), 732(m). ¹H NMR (400 MHz, $CDCl_3$ -d) δ 8.35(s, 1H), 7.75(s, 1H), 7.38–7.29(m, 1H), 7.19(s, 1H), 7.12(d, $J = 8.0$ Hz, 4H), 6.91(s, 1H), 6.72(s, 2H), 4.63(s, 2H), 3.65(s, 2H), 1.39(s, 6H). ¹³C NMR (101 MHz, $CDCl_3$ -d) δ 188.5, 175.6, 151.7, 138.3, 130.2, 129.6, 129.1, 124.5, 121.4, 82.3, 68.4, 38.1, 24.3. ESI-HRMS(m/z): Calcd. for $C_{19}H_{21}ClN_2O_3S$ [M+Na]⁺: 415.0895; found 415.0859.

Compound **17** Yield: 63%. IR (KBr, cm^{-1}): 3246(s), 2939(s), 1646(vs), 1513(vs), 1401(s), 1299(s), 1092(s), 963(m), 655(m). ¹H NMR (400 MHz, $CDCl_3$ -d) δ 8.17 (s, 1H), 7.31(s, 1H), 7.13(d, $J = 7.1$ Hz, 3H), 6.97(s, 2H), 6.91(s, 1H), 6.75(d, $J = 22.4$ Hz, 2H), 4.62(s, 2H), 3.70–3.57(m, 2H), 2.19(s, 3H), 1.39(s, 6H). ¹³C NMR (101 MHz, $CDCl_3$ -d) δ 186.3, 174.2, 153.1, 140.4, 137.6, 130.2, 129.6, 126.4, 125.9, 122.6, 86.5, 68.3, 37.6, 23.9, 23.2. ESI-HRMS(m/z): Calcd. for $C_{20}H_{23}ClN_2O_3S$ [M+Na]⁺: 429.1032; found 429.1016.

Compound **18** Yield: 74%. IR (KBr, cm^{-1}): 3246(s), 2991(s), 1666(vs), 1595(m), 1513(vs), 1487(s), 1248(s), 1168(s), 1034(s), 829(m), 734(m). ¹H NMR (400 MHz, $CDCl_3$ -d) δ 8.70(s, 1H), 8.03(s, 1H), 7.13(s, 2H), 7.00(d, $J = 8.2$ Hz, 2H), 6.79(s, 2H), 6.69(s, 2H), 4.60(s, 2H), 3.72(s, 1H), 3.66(s, 1H), 3.63(s, 3H), 1.37(s, 6H). ¹³C NMR (101 MHz, $CDCl_3$ -d) δ 186.8, 174.2, 157.4, 152.6, 133.1, 129.2, 127.6, 125.6, 121.8, 114.8, 84.2, 68.9, 56.7, 38.0, 23.6. ESI-HRMS(m/z): Calcd. for $C_{20}H_{23}ClN_2O_4S$ [M+H]⁺: 423.1167; found 423.1145.

4.3. H_2S measurement

A 5 mM solution of Na_2S in sodium phosphate buffer (20 mM, pH 7.4) was prepared ($Na_2S \cdot 9H_2O$, 120.20 mg in 100 mL volumetric flask) and used as the stock solution. Aliquots of 50, 100, 200, 400, 600, 800, 1000, 1500 μ L of the Na_2S stock solution were added into a 50 mL volumetric flask and dissolved in sodium phosphate buffer to obtain the standard solutions in 5, 10, 20, 40, 60, 80, 100, 150 μ M, respectively. 1 mL aliquot of the respective solution was reacted with the methylene blue (MB^+) cocktail: 30 mM $FeCl_3$ (200 μ L) in 1.2 M HCl, 20 mM of N,N -dimethyl-1,4-phenylenediamine sulfate (200 μ L) in 7.2 M HCl, 1% w/v of $Zn(OAc)_2$ (100 μ L) in H_2O at room temperature for at least 15 min (each reaction was performed in triplicate). The absorbance of methylene blue was measured at $\lambda_{max} = 670$ nm in UV-Vis

spectrophotometer (Lambda25). The Na₂S calibration curve was obtained.

The reaction was initiated by adding 15 µL of stock solution of the compounds (60 µM) into pH7.4 phosphate buffer (30 mL) containing accelerator for L-cysteine (1.0 mM). Then 2.0 mL of reaction aliquots were periodically taken and transferred to colorimetric cuvette containing zinc acetate (1%w/v, 200 µL) and N,N-dimethyl-1,4-

phenylenediamine sulfate (20 mM, 400 µL) in 7.2 M HCl and ferric chloride (30 mM, 400 µL) in 1.2 M HCl. The absorbance (670 nm) of the resulted solution was determined 15 min thereafter using an UV-Vis spectrometer (Lambda25). The H₂S concentration of each sample was calculated against a calibration curve of Na₂S.

4.4. Cytotoxicity assays

Cells were cultured in DMEM with 25 mmol/L glucose, which was supplemented with 10% (v/v) fetal bovine serum at 37 °C in a humidified atmosphere with 5% CO₂. Cells were routinely subcultured when grown to subconfluency (> 90% by visual estimate). Cell viability was determined using MTT assay. The cells (100 µL, 1 × 10⁵ cells mL⁻¹) were seeded into 96-well plates and left to adhere for 12 h. The media was removed from the wells and replaced with fresh media containing the compounds with different concentrations (25, 50, 100, 200, 400 and 800 µmol L⁻¹), respectively. The cells were then incubated for another 48 h before the incubation media were replaced with the complete medium and MTT (10 µL, 5 mg mL⁻¹ in phosphate buffer solution, PBS) was added to each well of the plate. The cells were further incubated for 4 h before the media were replaced with DMSO. Absorbance at 490 nm for each well of the plates was recorded with a microplate reader.

4.5. Protective effect of compounds on HUVEC injury induced by Ox-LDL

The HUVEC cells were pre-incubated with compounds at concentrations as indicated in text for 10 min before immediate exposure to Ox-LDL (100 µg/ml) stimulation. After treated with drugs for 24 h, cell viability was determined using MTT assay. In addition, the cells were washed gently with PBS for one time and incubated with Hoechst33342 (10 µg/mL), PI (10 µg/mL) and JC-1 (10 µg/mL) at 37 °C for 20 min, respectively. Then, the cells were washed once with PBS. Lastly, the cells were observed by fluorescent microscope (×200). The levels of bax, bcl-2 and caspase3 was performed according to the manufacturers' instructions. Briefly, cell were collected from 6-well plate immediately after lysed by RIPA Lysis Buffer and clarified by centrifugation at 12000 rpm for 10 min at 4 °C. The protein content was measured by BCA Protein Assay Kit. Finally, the content of bax, bcl-2 and caspase3 was detected by ELISA kit.

4.6. Oil red O staining

Cell culture was the same as above. Culture medium was removed, and cells were washed three times with PBS and fixed in 10% formalin for 30 min. Fixed cells were rinsed with PBS and then with 60% isopropanol for 5 min, and then stained with freshly prepared Oil Red O working solution for 20 min. Oil Red O working solution was removed. The nuclear were lightly stained with haematoxylin for 2 min. Stained cells were rinsed with distilled water and then observed using an inverted microscope (×200).

4.7. Analysis of cellular cholesterol ester contents

After the treatments, cells were washed twice with PBS, and total cellular lipids were extracted by incubating them for 30 min with hexane/isopropanol (3/2, v/v). Total intracellular cholesterol (TC), free cholesterol (FC) and triglyceride (TG) contents of the extracts were measured using enzymatic colorimetric tests, following the

manufacturer's instructions. The mass of cholesterol ester (CE) was calculated by subtracting FC from TC (FC plus CE). All results were normalized to total protein content measured using the bicinchoninic acid (BCA) protein assay.

4.8. Antioxidant assays

Cell culture was the same as above. The activities of SOD and the MDA content were measured using commercial kits following the manufacturer's instruction. Results were normalized to total protein content measured using the bicinchoninic acid (BCA) protein assay. The detection of ROS is done by staining the cells with DCFH-DA fluorescent probes. Dilute DCFH-DA in serum-free medium at 1:1000 to a final concentration of 10 µmol/L. Remove the cell culture medium and add the appropriate volume of diluted DCFH-DA. The volume to be added is preferably sufficient to cover the cells. Incubate for 20 min in a 37 °C cell incubator. The cells were washed three times with serum-free cell culture medium to sufficiently remove DCFH-DA which did not enter the cells. Finally, plate was observed and photographed under fluorescence microscope (×200). The densitometric analysis was performed using Image J software.

4.9. Anti-inflammatory assays

The levels of TNF-α and IL-10 was performed according to the manufacturers' instructions. Briefly, cell were collected from 6-well plate immediately after lysed by RIPA Lysis Buffer and clarified by centrifugation at 12000 rpm for 10 min at 4 °C. The protein content was measured by BCA Protein Assay Kit. The protein solution was added to a 96-well plate precoated with affinity-purified polyclonal antibodies specific for cytokines. An enzyme-linked polyclonal antibody specific for cytokines was added to the wells and left to react for 0.5 h and followed by a final wash to remove any unbound antibody-enzyme reagent. The intensity of the color was measured after addition of chromogen solution A, B stop solution and proportional to the amount of cytokines produced. The cytokines levels which in each sample was calculated from a standard curve generated with standard solution.

4.10. Western blot

The samples were then placed on ice, washed with ice-cold PBS, and lysed in RIPA lysis buffer for 30 mins. Lysates were clarified by centrifugation at 12000 rpm for 10 min at 4 °C, and the protein content in the supernatant was measured with a BCA Protein Assay Reagent Kit according to the manufacturer's instructions. Protein samples were separated by 10% sodium dodecyl sulfate-polyacrylamide gels and transferred onto polyvinylidene fluoride membranes. Next, membranes were blocked in 5% (w/v) dry milk powder in 0.1% Tris buffered saline/Tween 20 (TBST) for 1 h and incubated with primary antibodies at optimized dilutions at 4 °C overnight. Membranes were briefly washed and then incubated with secondary antibodies for another 1 h. Specific proteins were detected using a chemiluminescence kit. The densitometric analysis was performed using Image J software.

Declaration of Competing Interest

The authors confirm that this article content has no conflict of interest.

Acknowledgements

This work was financially supported by the National Natural Science Foundations of China (No. 21171079) and the Recruitment Program of Global Experts (1000 Talents Plan).

References

1. Lusis AJ. *Nature*. 2000;407:233–241.
2. Libby P, Ridker PM, Maseri A. *Circulation*. 2002;105:1135–1143.
3. Davignon J, Ganz P. *Circulation*. 2004;109:III-27–III-32.
4. Stocker R, Keaney Jr JF. *Physiol Rev*. 2004;84:1381–1478.
5. Sélley E, Kun S, Szijártó IA, et al. *Cardiovasc Diabetol*. 2014;13:69.
6. Kohn C, Schleifenbaum J, Szijartol A, et al. *PLoS ONE*. 2012;7:e41951.
7. Zhou Z, Rekowski M, Coletta C, et al. *Bioorg Med Chem*. 2012;20:2675–2678.
8. Li H, Mani S, Cao W, et al. *PLoS ONE*. 2012;7:e41614.
9. Yang G, Wu L, Jiang B, et al. *Science*. 2008;322:587–590.
10. Mani S, Li H, Untereiner A, et al. *Circulation*. 2013;127:2523–2534.
11. Wang Y, Zhao X, Jin H, et al. *Arterioscler Thromb Vasc Biol*. 2009;29:173–179.
12. Wen YD, Wang H, Kho SH, et al. *PLoS ONE*. 2013;8:e53147.
13. Zhang H, Guo C, Zhang A, et al. *Eur J Pharmacol*. 2012;697:106–116.
14. Pan LL, Liu XH, Gong QH, et al. *PLoS ONE*. 2011;6:e19766.
15. Gao M, Li J, Nie C, et al. *Bioorg Med Chem*. 2018;26:2632–2639.
16. Truong DH, Eghbal MA, Hindmarsh W, et al. *Drug Metab Rev*. 2006;38:733–744.
17. Liu Z, Han Y, Li L, et al. *Br J Pharmacol*. 2013;169:1795–1809.
18. Ross R, Harker L. *Science*. 1976;193:1094–1100.
19. Steiger AK, Marcatti M, Szabo C, et al. *ACS Chem Biol*. 2017;12:2117–2123.
20. Devarie-Baez NO, Bagdon PE, Peng B, et al. *Org Lett*. 2013;15:2786–2789.
21. Falk E. *J Am Coll Cardiol*. 2006;47:C7–C12.
22. Mitra S, Goyal T, Mehta JL. *Cardiovasc Drugs Ther*. 2011;25:419.
23. Mani S, Untereiner A, Wu L, et al. *Antioxid Redox Signal*. 2014;20:805–817.
24. Kataoka H, Kume N, Miyamoto S, et al. *Arteriosclerosis Thrombosis Vasc Biol*. 2001;21:955–960.
25. Riazy M, Chen JH, Steinbrecher UP. *Atherosclerosis*. 2009;204:47–54.
26. Eguchi K, Fujiwara Y, Hayashida A, et al. *Bioorg Med Chem*. 2013;21:3831–3838.
27. Bobryshev YV. *Micron*. 2006;37:208–222.
28. Xu S, Huang Y, Xie Y, et al. *Cytotechnology*. 2010;62:473–481.
29. Pignatelli P, Menichelli D, Pastori D, Violi F. *Kardiol Pol*. 2018;76:713–722.
30. Vanucci-Bacqué C, Camare C, Carayon C, et al. *Bioorg Med Chem*. 2016;24:3571–3578.
31. Morello F, Perino A, Hirsch E. *Cardiovasc Res*. 2008;82:261–271.
32. Yu XH, Zheng XL, Tang CK. *Adv Clin Chem*. 2015;70:1–30.
33. Loke WM, Proudfoot JM, Hodgson JM, et al. *Arterioscler Thromb Vasc Biol*. 2010;30:749–757.
34. Getz GS, Reardon CA. *Clin Lipidol*. 2014;9:657–671.
35. Choi KH, Kim JE, Song NR, et al. *Cardiovasc Res*. 2009;85:836–844.
36. Allahverdian S, Chehroudi AC, McManus BM, et al. *Circulation*. 2014;129:1551–1559.